Evidence for Universal Earthquake Rupture Initiation Behavior

Authors: Men-Andrin Meier[1], Thomas Heaton[1], John Clinton[2]

Affiliations:

[1]California Institute of Technology, Seismological Laboratory, Pasadena.

[2]Swiss Seismological Service, Swiss Federal Institute of Technology (ETH), Zurich.

Corresponding Author: Men-Andrin Meier (mmeier@caltech.edu), Caltech Seismological Laboratory, 1200 E California Blvd, Pasadena, CA 91125, (626) 395-6919

This article has been accepted for publication and undergone full peer review but has not been through the copyediting, typesetting, pagination and proofreading process which may lead to differences between this version and the Version of Record. Please cite this article as doi: 10.1002/2016GL070081

Abstract

Earthquake onsets provide a unique opportunity to study physical rupture processes because they are more easily observable than later rupture stages. Despite this relative simplicity, the observational basis for rupture onsets is unclear. Numerous reports of evidence for magnitude-dependent rupture onsets (which imply deterministic rupture behavior, e.g. *Colombelli et al.,* 2014) stand in contradiction to a large body of physics-based rupture modeling efforts, which are mostly based on inherently non-deterministic principles (e.g. *Rice*, 1993). Here we make use of the abundance of short-distance recordings available today; a magnitude-dependency of onsets should appear most prominently in such recordings. We use a simple method to demonstrate that all ruptures in the studied magnitude range ($4<M<8$) share a universal initial rupture behavior and discuss ensuing implications for physical rupture processes and earthquake early warning.

Key Points:

- We compare seismic near-source recordings in magnitude range 4<M<8
- Onsets of small and large earthquakes are statistically indistinguishable

Rupture onsets are not diagnostic of final rupture sizes

1 Introduction

What is it that decides whether an ongoing earthquake grows into a large rupture, tens or hundreds of kilometers long, involving several meters of peak slip and causing widespread destruction, or whether it stops to become another insignificant small event only perceived by highly sensitive instruments? This question lies at the heart of a debate on whether or not earthquakes develop in a deterministic and hence potentially predictable manner.

Numerous authors have suggested that the eventual size of an earthquake may be determined by the characteristics of rupture initiation (e.g. Iio 1995, Ellsworth & Beroza 1995; Olson & Allen 2005; Colombelli et al. 2014) e.g. because ruptures that start with a stronger initial push may be more likely to overcome mechanical barriers and thus may tend to propagate further (e.g. Heaton 1990). Most of these studies, however, have been contested on an observational basis (e.g. Mori & Kanamori 1996; Rydelek & Horiuchi 2006). Furthermore, the deterministic rupture development that rupture predictability implies would be surprising from the point of view of rupture mechanics and dynamics: Rupture processes are widely understood to be influenced by feedback mechanisms such as slip-rate dependent friction (Burridge & Knopoff 1967; Heaton 1990; Rice 1993), the - presumably heterogeneous - stress distribution along the rupturing fault (e.g. Smith & Heaton 2011), as well as the dynamics in the ongoing rupture energy budget (e.g. Aagaard & Heaton 2008; Elbanna & Heaton 2012), all of which render a deterministic rupture development improbable.

At least in part, this debate on rupture predictability is unresolved because the observational basis for the discussion is itself unclear, with different studies reporting different results. Reasons for the observational discrepancies may include that observational studies on rupture onsets have either analyzed narrow magnitude ranges (Iio 1992; Mori & Kanamori 1996;

Nakatani et al. 2000), have been based on small and often hand selected datasets (e.g. Ellsworth & Beroza 1995; Colombelli et al. 2014), have used indirect parameterizations of ground motion that are difficult to interpret (e.g. Olson & Allen 2005; Colombelli et al. 2014) and have focused on records with large hypocentral distances (Colombelli et al. 2014) which are strongly affected by attenuation that has to be corrected for, typically in simplistic ways.

If indeed rupture onsets are diagnostic of the future rupture development, initial differences between small and large earthquakes should appear most prominently in short distance recordings for which complicating effects from attenuation as well as from non-direct and shear-wave phases are minimal (Kanamori & Mori 2000). Today there are considerable amounts of such near-source recordings available for a wide magnitude range. From an observational point of view the debate should therefore be resolvable. To this end we have compiled a waveform data set that contains a majority of publicly available near-source records for large shallow crustal earthquakes, along with a large number of records from smaller events. Based on this data set we attempt to compile a model-free and objective description of ground motion onsets and search for significant differences between the onsets of small and large earthquakes.

2 Materials and Methods

2.1 Composite Near-Source Waveform Data Set

The data set consists of vertical ground motion records with hypocentral distances of $\leq$ 25km ("near-source", *Figure 1*). It includes all Japanese NIED strong motion records with $M_{JMA} \geq$ 4 ("K-NET & KiK-net", 2,471 records), the records from the Next Generation Attenuation West 1 data set that include P-wave onsets (Chiou & Youngs 2008) ("NGA West 1", 36 records), all strong motion and broadband records from the Southern California Seismic

Network with $M_L \geq 4$ ("SCSN", 568 records) as well as the near-source record from the 2008 Mw7.9 Wenchuan, China earthquake. A more detailed description of the data set is given as supplementary material.

2.2 Peak Absolute Ground Motion Displacement $pgd(t)$

For each record we identify the onset of ground motion using the SBPx P-phase picking algorithm (Meier et al. 2015) on the band-pass filtered acceleration traces. We numerically integrate all records to displacement time-series, $u(t)$, starting the integration 100 samples before the onset of the P-wave. We then process the displacement time series with a causal 2nd order Butterworth band-pass filter with corner frequencies of 0.075 and 30Hz. We choose an upper frequency limit well below the Nyquist frequency of the used records ($f_{Nyq} \geq 40$) in order to rule out any influence of acausal anti-alias filtering that is applied by modern data loggers (Scherbaum & Bouin 1997). We examine how peak absolute vertical displacements evolve over time for different magnitudes. We define $pgd(t') = \max\{|u(t)|\}$ the peak absolute amplitude of the ground motion displacement time-series during the time interval $t \in [t_{pick}\ t']$ where t_{pick} is the pick time and t' is increased in $0.01s$ intervals. For the sake of simplicity we do not account for the effects of radiation patterns, and we do not normalize the $pgd(t)$ amplitudes to a common distance.

Owing to the heterogeneous nature of our data set, pre-signal ambient noise levels before the earthquake signals vary strongly, from ~1e-6m/s^2 to ~1e-2m/s^2. The noise level can affect the $pgd(t)$-statistic, since high noise levels cause a detection delay of the signal onset (the time it takes for the signal to reach amplitudes above the noise level). In order to avoid artifacts from such noise-dependent detection delays, we ensure that all records have comparable

noise amplitudes by scaling up the noise levels of the low-noise signals to a common pre-signal amplitude level of 1e-3m/s^2 (95th percentile of the amplitude distribution, detailed description in supplementary material). *Supplementary Figure S1* shows the same figure as *Figure 2* without the noise scaling; it shows that the results of this study do not depend on the noise scaling procedure.

3 Results

3.1 Comparing $pgd(t)$ for Different Magnitudes

To compare the $pgd(t)$-statistic between small and large records we separate the data set into 6 magnitude bins. In each bin, and at each point in time *t'*, the $pgd(t)$ curves of individual records form an approximately log-normal amplitude distribution $D_{pgd}(t', M_{low} \leq \mathrm{M} < M_{up})$, where M_{low} and M_{up} are the lower and upper bounds of the magnitude bin, respectively. *Figure 2a* shows the temporal evolution of the median of the distribution in each magnitude bin.

During the initial $\sim 0.1 - 0.2s$ the median pgd curves are very steep, following a trend of $pgd \propto t^{\eta}$ with $\eta \sim 3$, where $\propto$ stands for proportionality. This high exponent implies a relatively gradual onset in the linear domain at short times. Note that the onset detection delay caused by the pre-signal noise reduces the observed slopes of the initial pgd curves. Without raising the noise levels on all records to 1e-3m/s^2, the exponent is even higher (*Figure S1*); this makes $\eta \sim 3$ a minimum estimate. The initial steep rise of $pgd(t)$ is not only a feature of the median curves but is observed in almost all individual records (*cf. Supplementary Figure S2*). These power-law shaped onsets represent the first displacement pulse in each seismogram. Small events, $\mathrm{M} < 5$, typically reach their final maximum P-wave

pgd value during this first pulse and their amplitudes only resume increasing once the direct S-phases arrive at 2-5 seconds (dots above abscissa in *Figure 2a*). The $pgd(t)$ curves of large events, on the other hand, keep growing as higher displacement amplitudes from later stages of the rupture (with larger amounts of slip) arrive at the recording station. While the initial growth occurs in typically smooth displacement pulses, the secondary $pgd(t)$ growth of the larger events is highly episodic, with repeated $pgd(t)$ bursts that can be several seconds apart. Furthermore, this later growth is characterized by a significantly lower rate ($\eta \sim 1.5$).

3.2 Kolmogorov-Smirnov Test

It is obvious from *Figure 2a* that, on average, small and large ruptures initially follow the same development. The large events start neither more nor less impulsively in the first tenths of a second. To examine at what point in time the amplitude distributions of different magnitude bins start to differ significantly we perform a two-sample Kolmogorov-Smirnov test (Massey 1951) at each time increment t'. *Figure 2b* shows the marginal p-values of these tests for neighboring magnitude bins. The p-value is an estimate of the probability to obtain the observed or a more extreme distance between two compared distributions if they have been sampled from the same parent distribution. It takes 5-6s for large magnitude events, D_{pgd} $(t', 6.5 \leq M < 8)$, to reach significantly higher peak displacement amplitudes than events in the D_{pgd} $(t', 6.0 \leq M < 6.5)$ bin. For the next smaller magnitude bins (D_{pgd} $(t', 5.5 \leq M < 6.0)$ vs. D_{pgd} $(t', 6.0 \leq M < 6.5)$) it takes a similar amount of time for significant differences to arise, although a deviation of the median curves is already observed at ~1s in *Figure 2a*. In either case this corresponds to a large fraction of the typical rupture duration of the smaller events of the comparison (e.g. Kanamori & Anderson 1975).

For events with short rupture durations the amplitude of the first displacement pulse is diagnostic of the event magnitude because the pulse reflect the entire rupture process. In fact, the often-employed predominant period parameters such as τ_c and τ_p^{max} (e.g. Allen & Kanamori 2003) presumably reflect the duration of this initial pulse (Kanamori 2005). For the larger magnitudes with much longer rupture growth, on the other hand, there is no correlation between initial displacement pulse amplitude (or duration) and final event size (*cf. Figure S1*).

4 Discussion and Conclusions

The observations presented in this study suggest that, at least for the magnitude range covered in this study, small and large ruptures start in indistinguishable ways. Significant differences arise only once the smaller events of the comparison have completed a large fraction of their eventual rupture process. This suggests that how large an earthquake is going to be is not dictated by what happens during the rupture onset. Observationally, this is consistent with reports from several of the largest earthquakes of the past decades which had rupture onsets that were highly similar to those of their foreshocks, including the 2011 Mw9.0 Tohoku, Japan (Hoshiba & Iwakiri 2011), the 2008 Mw7.9 Wenchuan, China (Peng et al. 2014) and the 1993 Mw7.3 Landers, California (Abercrombie & Mori 1994) earthquakes. Furthermore, this interpretation also agrees with what is predicted by an abundant body of dynamic rupture simulations (e.g. Lapusta and Rice, 2003; Gabriel et al. 2012) and source physics considerations (e.g. Murphy & Nielsen 2009; Kanamori & Mori 2000): that whether or not a rupture continues or stops is determined by the dynamic evolution of the ruptures' energy balance, as it propagates through a complex configuration of high and low stresses, fracture energy barriers and zones of variable resistance to slip.

Why, then, have numerous studies reported magnitude-dependent earthquake onsets? An important reason may be that most of the studies that argue for such a magnitude dependency have included long-distance recordings and may have misinterpreted path- for source-effects. It is a common practice to average all records from an earthquake to get rid of radiation pattern effects (e.g. Colombelli et al., 2014). This practice, however, is problematic for several reasons. First, at larger distances the onsets no longer correspond to direct P-phases and may therefore not be directly proportional to the moment rate function (Aki & Richards, 2002). Second, long distance recordings are much more numerous than short distance recordings, for simple geometrical reasons. They may then in fact dominate the average

estimate. Third, long distance waveforms may be strongly affected by attenuation. In fact, the Japanese JMA EEW system exploits the observation that long-distance recordings have systematically more gradual onsets to estimate epicentral distances for isolated sites where little other data is available (Doi 2011). The often-proposed magnitude-dependency of earthquake onsets should be most obvious in near-source recordings which are least contaminated by path effects. The fact that such recordings show no sign of such a tendency suggests that an observed magnitude dependency in long-distance recordings is only an apparent effect, stemming from the wave-path rather than from the source.

Furthermore, there is a distinct change in pgd growth rates around 0.1-0.2s where the pgd evolution changes from $pgd \propto t^{\sim 3}$ to $pgd \propto t^{\sim 1.5}$. Neither the initial growth rates with $\eta \sim 3$ nor the growth rates of $\eta \sim 1.5$ at later stages are consistent with simple standard shear crack models with constant rupture velocity and constant stress drop: these models predict $pgd \propto t^2$ (e.g. Sato & Hirasawa 1973). Somewhat counter-intuitively, the high initial power law exponents imply low initial potency rates, since high order power laws have very gradual onsets at short time scales. There are two candidate explanations for these low initial potency rates and the subsequent change in scaling. They may either reflect an initial period over which the rupture velocity v_r grows towards its steady-state value (Sato & Kanamori 1999; Deichmann 1997). Alternatively, the actual potency rates may be growing as $pgd \propto t^{\sim 1.5}$ from the very beginning but anelastic attenuation may cause the observed displacement pulses to appear more gradual than the actual potency rate function itself (e.g. Kanamori & Anderson 1977; Mori & Kanamori 1996).

In the former case, the rupture area S of small earthquakes would be smaller than what is typically inferred under the assumption of a constant v_r. This would imply that an observed

seismic moment would have to be generated over a smaller area and hence, the smaller events would be characterized by higher stress drops. Conventional stress drop analyses (e.g. Shearer et al., 2006) would not resolve such a trend since they are based on the assumption of constant v_r. Systematically higher stress drop for small events would be consistent with the idea that ruptures nucleate in locations of high stress concentrations, and it would reconcile the high shear stresses needed to start ruptures in laboratory studies (hundreds of MPa) with real-earth observations. More fundamentally, however, it would introduce a scaling break between the larger earthquakes whose average v_r is close to the steady-state value and the smaller earthquakes for which the period of below-steady-state v_r makes up a large fraction of the total rupture duration. The spatial scale where this break occurs would be on the order of the rupture area of a M4-5 earthquake (several hundred meters), i.e. it would be much smaller than the thickness of the seismogenic crust. A viable physical origin of the scaling break could be a transition from a crack-like to pulse-like rupture mechanism. In fact, most dynamic simulations of pulse-like rupture have accelerating crack-like nucleation that transitions to pulse-like at a length scale that is controlled by the characteristics of the evolution between static and dynamic frictions (e.g. Aagaard and Heaton, 2001).We therefore speculate that the observed scaling change of pgd at 0.1-0.2 sec may be a consequence of such a transition and propose a rupture model in which the rupture mechanism transitions from an initial crack mode with accelerating v_r, to a pulse mode in which v_r may be variable but no longer systematically increases with time, and in which the constant average slip-to-length ratio develops that is observed in large earthquakes (*Figure 3*).

On the other hand, a duration of ~0.1s is also consistent with the time over which signal may be affected by attenuation, as modeled with the attenuation operator of Futterman 1962, using a high near-surface attenuation quality factor of ~200 and a recording distance of ~20km,

suggesting that the observed high power law exponents might simply be an apparent rather than a source effect. While our observations clearly demonstrate that the data is incompatible with the concept of deterministic rupture evolution further research is needed to establish whether the data support or contradict the often-presumed scale invariance of earthquake rupture characteristics.

From a practical perspective, the result that small and large earthquakes have indistinguishable onsets has the negative implication that it will not be possible to use waveform onset observations to predict how large an earthquake is going to be once its initiation has been observed. Some existing Earthquake Early Warning (EEW) systems have been built on this premise and may need to be modified. It is to be noted, however, that such rupture predictability is not a prerequisite for timely EEW alerts. Even if only the rupture that has already occurred can be quantified, strong ground motions can be predicted before they arrive at sufficiently distant sites (e.g. Böse et al. 2012), although warning times would generally be longer if future rupture evolution could be predicted. What is important is that this incapacity to predict future rupture development is accounted for in EEW system design (Meier et al. 2015), in that the algorithms need to consider (and quantify) the probability that an ongoing rupture may grow beyond its current size.

Acknowledgements

We are grateful to Hiroo Kanamori, Nadia Lapusta, Jean-Paul Ampuero, Nicolas Deichmann, Shunta Noda, Yannik Behr, Alice Gabriel, Stephen Perry and Natalie Higgins for discussions that helped to advance this project, and to Chaoyong Peng for the help with the Wenchuan earthquake data. This work was partly funded by ETH Zurich ETHIIRA grant ETH-22 10-3.

Data

The Japanese waveform data can be downloaded from http:// www.kik.bosai.go.jp/ (last accessed August 2015). We used the Seismic Transfer Program tool from http://scedc.caltech.edu/research-tools/ stp-index.html (last accessed September 2014) to retrieve southern California waveform, catalog, and arrival time data. The Next Generation Attenuation-West 1 waveform and metadata were obtained from http://peer.berkeley.edu (last accessed March 2014). The Wenchuan record was obtained from http://222.222.119.9/index.asp (last accessed June 2015). The SBPx-algorithm was published as *SBPx.m* on mathworks.com/matlabcentral/fileexchange/ (last accessed July 2015).

References

Aagaard, B.T., Heaton, T.H. & Hall, J.F., 2001. Dynamic Earthquake Ruptures in the Presence of Lithostatic Normal Stresses : Implications for Friction Models and Heat Production. , (December), pp.1765–1796.

Aagaard, B.T. & Heaton, T.H., 2008. Constraining fault constitutive behavior with slip and stress heterogeneity. *Journal of Geophysical Research: Solid Earth*, 113(4), pp.1–18.

Abercrombie, R. & Mori, J., 1994. Local Observations of the Onset of a Large Earthquake - 28 June 1992 Landers, California. *Bulletin of the Seismological Society of America*, 84(3), pp.725–734.

Allen, R.M. & Kanamori, H., 2003. The potential for earthquake early warning in southern California. *Science*, 300(5620), pp.786–789.

Böse, M., Heaton, T.H. & Hauksson, E., 2012. Real-time finite fault rupture detector (FinDer) for large earthquakes. *Geophysical Journal International*, 191(2), pp.803–812.

Burridge, R. & Knopoff, L., 1967. Model and theoretical seismicity. *Bulletin of the Seismological Society of America*, 57(3), pp.341–371.

Chiou, B.-J. & Youngs, R.R., 2008. An NGA model for the average horizontal component of peak ground motion and response spectra. *Earthquake Spectra*, 24(1), pp.173–215.

Colombelli, S. et al., 2014. Evidence for a difference in rupture initiation between small and large earthquakes. *Nature Communications*, 5.

Deichmann, N., 1997. Far-field pulse shapes from circular sources with variable rupture velocities. *Bulletin of the Seismological Society of America*, 87(5), pp.1288–1296.

Doi, K., 2011. The operation and performance of Earthquake Early Warnings by the Japan Meteorological Agency. *Soil Dynamics and Earthquake Engineering*, 31(2), pp.119–126.

Elbanna, A.E. & Heaton, T.H., 2012. A new paradigm for simulating pulse-like ruptures: The

pulse energy equation. *Geophysical Journal International*, 189(3), pp.1797–1806.

Ellsworth, W.L. & Beroza, G.C., 1995. Seismic evidence for an earthquake nucleation phase. *Science (New York, N.Y.)*, 268(5212), pp.851–855.

Frank J. Massey, J., 1951. Kolmogorov-Smirnov Test for Goodness of Fit. *Test*, 46(253), pp.68– 78.

Futterman, W.I., 1962. Dispersive body waves. *Journal of Geophysical Research*, 67(13), pp.5279-5291.

Gabriel, A.-A. et al., 2012. The transition of dynamic rupture styles in elastic media under velocity-weakening friction. *Journal of Geophysical Research: Solid Earth*, 117(B9).

Heaton, T., 1990. Evidence for and implications of self-healing pulses of slip in earthquake rupture. *Physics of the Earth and Planetary Interiors*.

Hoshiba, M. & Iwakiri, K., 2011. Initial 30 seconds of the 2011 off the Pacific coast Tohoku earthquake (M w 9 . 0) – amplitude and τc for magnitude estimation for earthquake early warning -. *Earth Planets Space*, 63, pp.553–557.

Iio, Y., 1995. Observations of the slow initial phase generated by microearthquake nucleation and propagation. *Journal of Geophysical Research*, 100(B8), pp.15333–15349.

Iio, Y., 1992. Slow initial phase of the P-wave velocity pulse generated by microearthquakes. *Geophysical Research Letters*, 19(5), pp.477–480.

Kanamori, H., 2005. Real-Time Seismology and Earthquake Damage Mitigation. *Annual Review of Earth and Planetary Sciences*, 33(1), pp.195–214.

Kanamori, H. & Anderson, D.L., 1977. Importance of physical dispersion in surface wave and free oscillation problems: Review. *Reviews of Geophysics*, 15(1), pp.105–112.

Kanamori, H. & Anderson, D.L., 1975. Theoretical basis of some empirical relations in seismology. *Bulletin of the Seismological Society of America*, 65(5), pp.1073–1095.

Kanamori, H. and Mori, J., 2000. Microscopic processes on a fault plane and their

implications for earthquake dynamics. *Problems in geophysics for the new millennium*. Bolònia: Editrice Compositori, pp.73-88.

Lapusta, N. and Rice R. R., 2003. Nucleation and early seismic propagation of small and large events in a crustal earthquake model. *Journal of Geophysical Research*, 108, pp.1–18, doi:10.1029/2001JB000793

Meier, M.-A., Heaton, T. & Clinton, J., 2015. The Gutenberg Algorithm: Evolutionary Bayesian Magnitude Estimates for Earthquake Early Warning with a Filter Bank. *Bulletin of the Seismological Society of America*, 105(5), pp.2774–2786.

Mori, J. & Kanamori, H., 1996. Initial rupture of earthquakes sequence in the 1995 Ridgecrest, California sequence. *Geophysical Research Letters*, 23(18), pp.2437–2440.

Murphy, S. & Nielsen, S., 2009. Estimating Earthquake Magnitude with Early Arrivals: A Test Using Dynamic and Kinematic Models. *Bulletin of the Seismological Society of America*, 99(1), pp.1–23.

Nakatani, M., Kaneshima, S. and Fukao, Y., 2000. Size-dependent microearthquake initiation inferred from high-gain and low-noise observations at Nikko district, Japan. *Journal of Geophysical Research*, 105(B12), pp.28095-28109.

Olson, E.L. & Allen, R.M., 2005. The deterministic nature of earthquake rupture. *Nature*, 438(7065), pp.212–215.

Peng, C. et al., 2014. Early magnitude estimation for the MW7.9 Wenchuan earthquake using progressively expanded P-wave time window. *Scientific Reports*, 4, p.6770.

Rice, J.R., 1993. Spatio-temporal complexity of slip on a fault. *Journal of Geophysical Research*, 98(B6), p.9885.

Rydelek, P. & Horiuchi, S., 2006. Earth science: Is earthquake rupture deterministic? *Nature*, 442(7100), pp.E5–E6.

Sato, T. & Hirasawa, T., 1973. Body wave spectra from propagating shear cracks. *Journal of*

Physics of the Earth.

Sato, T. & Kanamori, H., 1999. Beginning of Earthquakes Modeled with the Griffith's Fracture Criterion. *Bulletin of the Seismological Society of America*, 89(1), pp.80–93.

Scherbaum, F. & Bouin, M.P., 1997. FIR filter effects and nucleation phases. *Geophysical Journal International*, 130(3), pp.661–668.

Smith, D.E. & Heaton, T.H., 2011. Models of stochastic, spatially varying stress in the crust compatible with focal-mechanism data, and how stress inversions can be biased toward the stress rate. *Bulletin of the Seismological Society of America*, 101(3), pp.1396–1421.

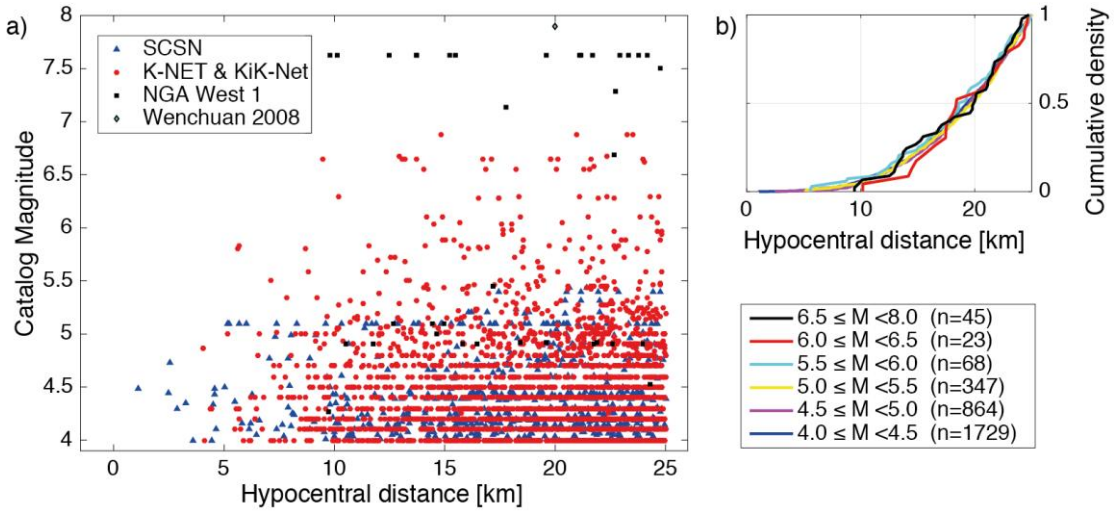

Figure 1 **Data set overview**. (a) Magnitudes and hypocentral distances of the records used in this study from the four data sources. (b) Empirical cumulative hypocentral distance distributions for the records in 6 magnitude bins and number of records, n, in each bin.

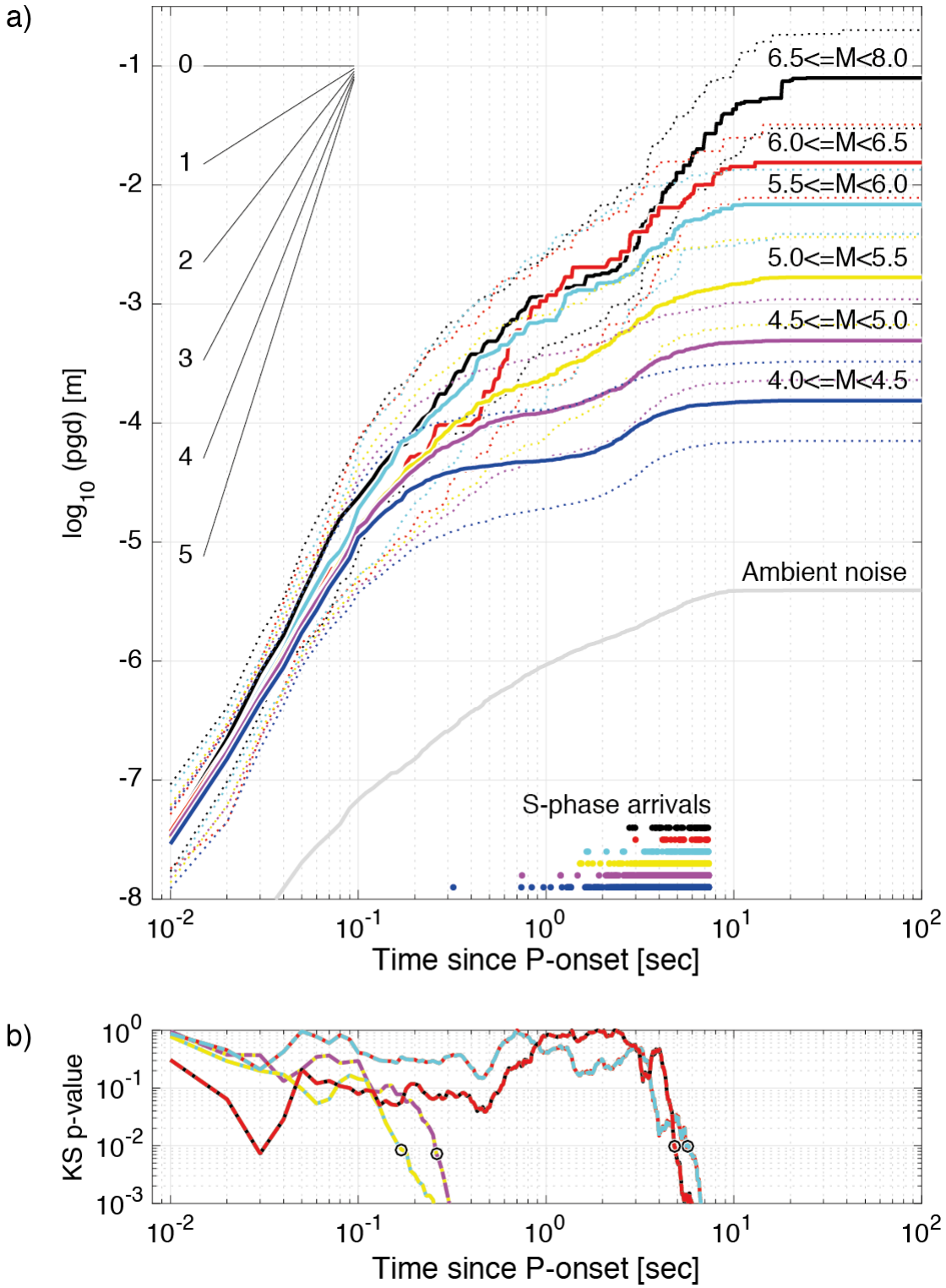

Figure 2 **Temporal evolution of pgd(t).** (a) Medians (solid lines) and 5^{th}/95^{th} percentiles (dotted lines) of the pgd(t) distributions in 6 magnitude bins. The dots above the abscissa show theoretical arrival times of the direct S-phases. Gray line gives median of the pgd(t) statistic computed on randomly selected ambient noise segments. (b) Asymptotic p-values of a two-sample Kolmogorov-Smirnov test for neighboring magnitude bins. Black circles indicate the time when the p-value drops below 1%. The p-values of the comparison of the lowest two magnitude bins is close to zero from the beginning and do not appear on the plot.

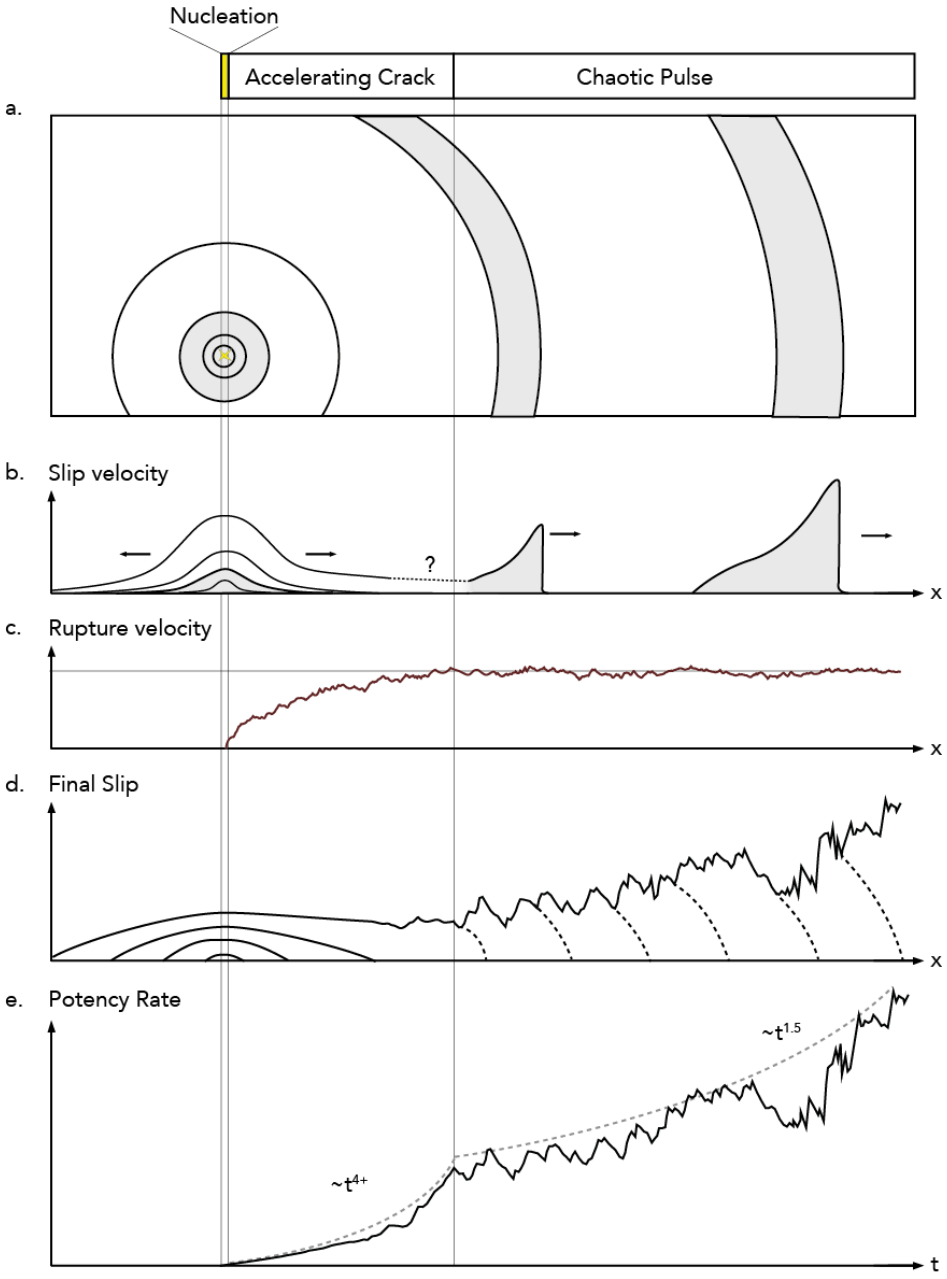

Figure 3 **Conceptual rupture model sketch.** Front view (a) of the proposed rupture model that transitions from crack-like to pulse-like rupture once steady-state rupture velocity is reached. (b) Slip velocity, (c) rupture velocity v_r and (d) final slip amplitudes as a function of distance along the fault; (e) potency rate as a function of time since rupture onset, with a power law envelope with a high exponent during the period of increasing v_r and a lower exponent during the pulse-phase with steady-state v_r.